Numerical study of aerosol particle sampling from a low-speed flow

A.A. Medvedev

Research & Development Center of Aerobiology,
State Scientific Center of Virology and Biotechnology "Vektor," Koltsovo, Novosibirsk Region

Received March 11, 2002

Sampling of aerosol particles in a thin-walled tube opposite in direction to an external air flow is studied numerically using a solution of the Navier–Stokes equation, integration of equation of particle motion, and calculation of aspiration efficiency. Of primary concern is the case when the speed of a free air flow is much lower than the mean sampling velocity. It is shown that, when the velocity ratio tends to zero, the aspiration efficiency is determined by particle deposition on the tube walls and depends only on the Stokes number. Based on the calculation results, a semiempirical formula is derived for the aspiration efficiency as a function of the Stokes number and velocity ratio. The results of the calculations and the derived semiempirical formula can be used to choose the regimes of aerosol sampling from ambient air.

Introduction

Aerosol study most frequently begins with pumping of air containing the aerosol particles into some measuring device with the use of some sampler. The simplest and most frequently used sampler is a thin-walled cylindrical tube. During sampling from the near-ground atmospheric layer, the wind speed constantly changes, often resulting in a situation when the speed of the external flow is much lower than the air speed at the tube nozzle. In addition, the flow pumped into the nozzle is accelerated while the direction of particle motion is deflected from air flow lines. As a consequence, the aerosol disperse composition can be distorted, and a measure of the distortion serves the aspiration efficiency $A = c/c_0$, where c and c_0 are flux concentrations of a given aerosol fraction inside the tube and in the external flow, respectively. To minimize the aspiration distortions, the tube is oriented in the direction opposite to the velocity vector of the external flow.

To estimate the efficiency of aspiration into the counter-flow tube, of common use is the semiempirical formula of Belyaev and Levin,[1,2] inferred from experimental data:

$$A = 1 + (R-1)\left[1 - \frac{1}{1 + \left(2 + \frac{0.62}{R}\right)\mathrm{Stk}}\right], \qquad (1)$$

where $R = W/V_0$ is the velocity ratio; W is the external flow velocity; V_0 is the mean air speed in the tube; $\mathrm{Stk} = \tau W/D$ is the Stokes number, D is the tube inner diameter, and τ is the time of particle relaxation. The authors of Refs. 1 and 2 have photographed the trajectories of individual particles and determined the diameter Φ of the tube of limiting trajectories in an unperturbed flow. By the limiting trajectories are meant the ones establishing a line of demarcation between the particles entered into the tube nozzle and those past by the nozzle. The efficiency of aspiration was then determined from the relation

$$A = \frac{\Phi^2}{D^2} R, \qquad (2)$$

obtained for the condition of conservation of the particle flow inside the tube of limiting trajectories.

Formula (1) describes approximately the data obtained for $R > 0.17$; and in this range, it fits well the published experimental data and theoretic calculations. For smaller R values, the published data are inconsistent.

The results of Refs. 3 and 4, also obtained with the method of limiting trajectories, well agree with Eq. (1) up to $R = 0.03$, however, substantially diverging from experimental data.[5,6] It can be easily seen that, as R tends to zero for a constant Stk value, for example, during increasing rate of aspiration to the nozzle, the efficiency of aspiration tends to zero according to Eq. (1). At the same time, the experimental data[5,6] demonstrate a qualitatively different, nonmonotone behavior of the aspiration efficiency, which decreases with decreasing R, reaches its minimum, and then again increases. In Refs. 3 and 4 this discrepancy is explained by the fact that the particles bounced off the tube's outer surface could be then pumped into the tube thus increasing the aspiration efficiency, measured in Refs. 5 and 6 by comparing the particle concentration at the tube nozzle and independently measured concentration in the flow. At the same time, data of Refs. 1–4 are unaffected by the secondary aspiration because the limiting particle trajectories were recorded visually.

In a number of papers, the aspiration of particles to a tube was studied theoretically. In Ref. 7, a model

0235-6880/02/08 663-04 $02.00

of point sink is used to calculate the air velocity field; it is shown that, as the external flow's rate decreases, the efficiency of aspiration tends to unity. It should be noted that in the model used there, the influence of tube walls was not taken into consideration. In Refs. 8 and 9, the air velocity field nearby the tube was calculated by solving the Navier–Stokes equations. Then, integration of equations of particle motion in the obtained air velocity field was used to determine the limiting particle trajectories and aspiration efficiency. The results of Refs. 8 and 9 well agree with Eq. (1) for $R > 0.2$; at the same time, the results of Ref. 9 show a certain disagreement at $R = 0.1$. It should be noted that the lower limit of the studied range of R was taken to be 0.2 in Ref. 8 and 0.1 in Ref. 9.

The question how the aspiration efficiency behaves at small velocity ratios is practically important for correct choice of sampler operation conditions and analysis of obtained results. The efficiency of aspiration is affected by many factors; they include inertia, particle impaction on the tube wall, gravitational sedimentation, and loss of particles inside the tube. The gravitational forces can be neglected, provided the external flow rate is much larger than the particle sedimentation rate. The particle impaction contributes a significant uncertainty since it depends on interaction of particles with tube walls. To estimate the range of this uncertainty, some other factors should be correctly taken into account. At the same time, data on influence of the particle inertia on the behavior of the aspiration efficiency at $R < 0.2$ are insufficient. The purpose of this work is a numerical study of the efficiency of aspiration to the tube nozzle at small values of the velocity ratio, taking into account only the effects of particle inertia.

1. Method

The procedure of finding the aspiration efficiency included the following steps. First, the field of velocities of an air flow free of particles was calculated; and then, the particle trajectories were determined.

The flow velocity field was calculated by solving the Navier–Stokes equations for stationary axially symmetric current of the viscous incompressible air in the cylindrical coordinate system:

$$\rho\left(v_r'\frac{\partial v_r'}{\partial r'}+v_z'\frac{\partial v_r'}{\partial z'}\right)=$$

$$=-\frac{\partial P}{\partial r'}+\mu\left(\frac{\partial^2 v_r'}{\partial r'^2}+\frac{1}{r'}\frac{\partial v_r'}{\partial r'}-\frac{v_r'}{r'^2}+\frac{\partial^2 v_r'}{\partial z'^2}\right); \qquad (3)$$

$$\rho\left(v_r'\frac{\partial v_z'}{\partial r'}+v_z'\frac{\partial v_z'}{\partial z'}\right)=$$

$$=-\frac{\partial P}{\partial z'}+\mu\left(\frac{\partial^2 v_z'}{\partial r'^2}+\frac{1}{r'}\frac{\partial v_z'}{\partial r'}+\frac{\partial^2 v_z'}{\partial z'^2}\right), \qquad (4)$$

closed using the continuity equation

$$\frac{\partial v_r'}{\partial r'}+\frac{v_r'}{r'}+\frac{\partial v_z'}{\partial z'}=0, \qquad (5)$$

where v_r' and v_z' are air velocity components; P is the pressure; ρ and μ are the air density and viscosity.

Equations (3)–(5) were rewritten in terms of variables "vortex –current function":

$$r^2\left[\frac{\partial}{\partial r}\left(\frac{w}{r}\frac{\partial\psi}{\partial z}\right)-\frac{\partial}{\partial z}\left(\frac{w}{r}\frac{\partial\psi}{\partial r}\right)\right]=$$

$$=\frac{1}{\mathrm{Re}}\left[\frac{\partial}{\partial r}\left(r^3\frac{\partial(w/r)}{\partial r}\right)+\frac{\partial}{\partial z}\left(r^3\frac{\partial(w/r)}{\partial z}\right)\right]; \qquad (6)$$

$$\left(\frac{w}{r}\right)r=-\frac{\partial}{\partial r}\left(\frac{1}{r}\frac{\partial\Psi}{\partial r}\right)-\frac{\partial}{\partial z}\left(\frac{1}{r}\frac{\partial\Psi}{\partial z}\right). \qquad (7)$$

The intensity of the vortex (w/r) and the function of current Ψ were defined as:

$$\frac{w}{r}=\frac{1}{r}\left(\frac{\partial v_z}{\partial r}-\frac{\partial v_r}{\partial z}\right); \qquad (8)$$

$$v_z=-\frac{1}{r}\frac{\partial\Psi}{\partial r},\quad v_r=\frac{1}{r}\frac{\partial\Psi}{\partial z}, \qquad (9)$$

where

$$v_z=\frac{\partial v_z'}{V_0},\quad v_r=\frac{\partial v_r'}{V_0};\quad r=\frac{r'}{D};\quad z=\frac{z'}{D} \qquad (10)$$

are the velocity and coordinates, made dimensionless with the use of mean air velocity V_0 in the tube and the tube inner diameter D as the scales; $\mathrm{Re}=\rho V_0 D/\mu$ is the Reynolds number.

Equations (6) and (7) were transformed into finite-difference form and solved using the iteration technique as given in Ref. 10.

The calculation region shown in Fig. 1 represents a cylinder whose axis coincides with the tube axis of symmetry. The air flow enters the region through the end surface *ab* of the cylinder, and leaves it through the inner cross-section *dh* and outer cross-section *gc*. It is assumed that at the input *ab* and lateral *bc* boundaries of the calculation region the flow is unperturbed and the flow rate is equal to the external flow rate.

At the tube wall surface and axis of symmetry, the function of current is constant. Since the function of current is defined as accurate to an additive constant factor, at the tube surface it was assumed to be zero. Its values for the boundaries *ab*, *ad*, and *bc* were precalculated by integrating (9) and (10) for air velocity profiles set above:

$$\Psi_{ad}=0.125,\quad \Psi_{ab}(r)=0.125-Rr^2/2,$$

$$\Psi_{bc}=0.125-RS^2/2,$$

where S is the radius of the calculation region. The intensity of the vortex at the boundaries *ab* and *bc* was equal to zero. These values do not change during the

iteration procedure, in contrast to the intensity of vortex at the tube wall surface and at the symmetry axis calculated at each iteration step by the finite-difference formulae. At the exit boundaries *gc* and *dh* of the region, the velocity distribution was unknown. It was only assumed that the radial component of air velocity at the boundaries was zero, i.e., the lines of current were parallel to the tube axis. Thus, at each iteration step, the function of current and vortex at the exit boundaries were set equal to the corresponding values at the upstream grid points.

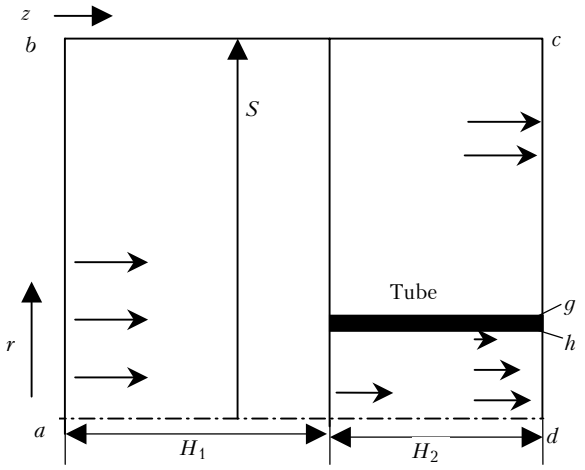

Fig. 1. Calculation region for air flow field near tube.

After the function of current is calculated at each finite-difference grid point, the velocity can be determined using relations (9) and (10). The equations of particle motion are written in accordance with the Stokes law:

$$\mathrm{Stk}\,\frac{\mathrm{d}^2 r}{\mathrm{d}t^2} = v_r - \frac{\mathrm{d}r}{\mathrm{d}t}, \qquad (11)$$

$$\mathrm{Stk}\,\frac{\mathrm{d}^2 z}{\mathrm{d}t^2} = v_z - \frac{\mathrm{d}z}{\mathrm{d}t}. \qquad (12)$$

The particle trajectories were calculated by integrating the equations of particle motion using the Runge–Kutta method of the fourth order. Initial points of the trajectories were located at the boundary *ab*. The initial particle velocity was equal to the external flow velocity W.

As in many papers on aspiration (see, e.g., Ref. 1), we considered the efficiency of aspiration as a function of dimensionless similarity parameters, namely, the Stokes number and velocity ratio. The calculations were made at a fixed number Re = 1000. Precalculations, as well as data of Ref. 8, show that the efficiency of aspiration weakly depends on the Reynolds number in the range $500 < \mathrm{Re} < 10000$.

Figure 2 shows the limiting line of the air current pumped into the tube (solid line) and particle trajectories (dashed lines) calculated at $R = 0.02$ and Stk = 2. Particles having touched the tube wall were excluded from the sample. Particles passing the cross-section of the tube nozzle were assumed as sampled. The limiting trajectories were determined by the bisection method. The efficiency of aspiration was calculated by formula (2).

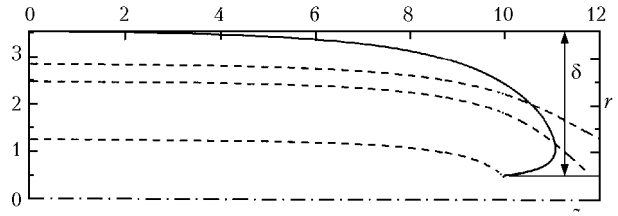

Fig. 2.

In the calculations, the sizes of calculation domain and the number of grid points were chosen so that their further increase did not influence the calculated aspiration efficiency. The length of the calculation domain was equal to twenty tube diameters in the flow direction and ten tube diameters downward the tube nozzle ($H_1 = 20$, $H_2 = 10$). The tube wall's thickness was equal to minimal grid step because its influence on the aspiration efficiency was not a subject of this work. The radius of calculation domain ($S = 16$) was taken sufficiently large for the air flow pumped into the tube was less than 5% of the total flow entering the region. The number of grid points was 91 in the radial direction and 109 in the direction of the tube axis. To gain a better approximation, the finite-difference grid had nonuniform grid spacing, denser near tube wall and nozzle, where the velocity and pressure gradients are maximal.

2. Results

After completion of preliminary studies, we performed a series of calculations in which the efficiency of aspiration was determined as a function of velocity ratio $R = 0.02$–0.9 and the Stokes number Stk = 0.01–2. The lower limit of the velocity ratio range was chosen so that the influence of gravitational sedimentation could be neglected for typical aspiration rates and particle sizes. For instance, at $V_0 = 10$ m/s and $R = 0.02$, the external flow rate is $W = 0.2$ m/s, that is far in excess of sedimentation rate of particles with diameter of 10 μm (0.003 m/s). The results of calculations shown by dots in Fig. 3 well agree with semiempirical equation (1) at $W/V_0 > 0.2$, except the $W/V_0 < 0.2$ case, when a significant disagreement is observed.

The aspiration losses can be considered as a result of particle sedimentation on an imaginary ring of δ thickness outside the tube (see Fig. 2). The ring's internal diameter equals to the tube diameter, while its external diameter coincides with the diameter of the cylinder of limiting air flow lines in an unperturbed flow. The general expression for aspiration efficiency is[2]

$$A = 1 + \alpha\,(R - 1), \qquad (13)$$

where α is a dimensionless parameter, which can be interpreted as the efficiency of sedimentation on the ring.

Reference 11 suggests the following expression for efficiency of particle sedimentation on bodies of different shapes:

$$\alpha = 1 - \frac{1}{1 + k\ \mathrm{St}}, \qquad (14)$$

where k is dimensionless parameter dependent on the obstacle shape; St is the modified Stokes number defined here as the ratio of the distance τW, at which the particle is coming to a halt, to the obstacle width δ.

Using the diameter of the limiting surface of the air flow, determined from relation (2), and assuming that the efficiency of aspiration $A = 1$, we obtain the following expression for the ring width:

$$\delta = D\,\frac{1 - \sqrt{R}}{2\sqrt{R}} \qquad (15)$$

and for the modified Stokes number

$$\mathrm{St} = \frac{\tau W}{\delta} = 2\mathrm{Stk}\,\frac{\sqrt{R}}{1 - \sqrt{R}}. \qquad (16)$$

Combination of Eqs. (13), (14), and (16) yields

$$A = 1 + \left[1 - \left(1 + 2k\ \mathrm{Stk}\,\frac{\sqrt{R}}{1 - \sqrt{R}}\right)^{-1}\right](R - 1). \qquad (17)$$

By fitting Eq. (17) to calculated values of the aspiration efficiency, we obtained the following relation for the coefficient k:

$$k = \frac{1}{2} + 2\left(\frac{1 - \sqrt{R}}{\sqrt{R}}\right). \qquad (18)$$

Use of Eq. (18) in Eq. (17) gives the semiempirical equation for the aspiration efficiency

$$A = 1 + \left[1 - \left(1 + \mathrm{Stk}\,\frac{\sqrt{R}}{1 - \sqrt{R}} + 4\mathrm{Stk}\right)^{-1}\right](R - 1). \qquad (19)$$

In Fig. 3, solid lines show the dependences of the aspiration efficiency on R, calculated for several Stk values from Eq. (19); dots show values of the aspiration efficiency determined numerically, and the dashed lines are calculated from Eq. (1). As is seen, Eq. (19) well fits the numerical values obtained for $\mathrm{Stk} \geq 0.2$, and satisfactorily fits them for smaller values of the Stokes number.

From the obtained results we can conclude the following. For a constant Stokes number, i.e., for a constant wind velocity, the efficiency of aspiration decreases with increasing aspiration rate; and as $R \to 0$, it tends to a constant value, determined by the rate of particle deposition on the tube wall and the Stokes number:

$$A = \frac{1}{1 + 4\mathrm{Stk}}. \qquad (20)$$

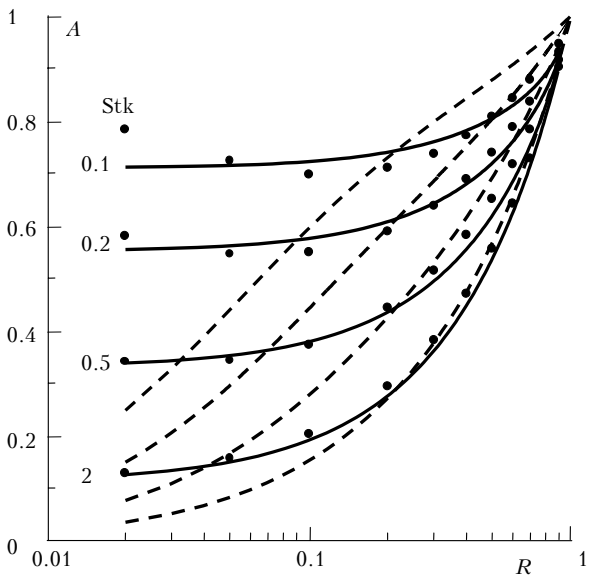

Fig. 3. Efficiency of aspiration as a function of velocity ratio R and the Stokes number.

Model of point sink[7] takes into account only capture of particles by velocity field of the pumped air. For the tube, the efficiency of aspiration can be represented as a difference between efficiency of aspiration to the point sink and efficiency of particle deposition on the tube wall. It should be noted that Eq. (20) can readily be derived from Eqs. (13) and (14) by taking into account parameter $k = 4$, as obtained in Ref. 11 for particle deposition on the surface of the cylinder. From Eq. (20) it follows that $A > 0.9$ at $\mathrm{Stk} < 0.1$. This result can be used as a criterion of undistorted sampling.

References

1. S.P. Belyaev and L.M. Levin, Izv. Akad. Nauk SSSR, Ser. Fiz. Atmos. Okeana **6**, No. 11, 1137–1152 (1970).
2. S.P. Belyaev and L.M. Levin, J. Aerosol Sci. **5**, 325–338 (1974).
3. G.N. Lipatov, S.A. Grinshpun, G.L. Shingaryov, and A.G. Sutugin, J. Aerosol Sci. **17**, 763–769 (1986).
4. S.A. Grinspun, G.N. Lipatov, A.G. Sutugin, Aerosol Sci. and Technol. **12**, 716–740 (1990).
5. H. Gibson and T.L. Ogden, J. Aerosol Sci. **8**, 361–365 (1977).
6. C.N. Davies and M. Subari, J. Aerosol Sci. **13**, 59–71 (1982).
7. L.M. Levin, Izv. Akad. Nauk SSSR, Ser. Geofiz., No. 7, 914–925 (1957).
8. D.J. Rader and V.A. Marple, Aerosol Sci. and Technol. **8**, 283–299 (1988).
9. B.Y.H. Liu, Z.Q. Zhang, T.H. Kuehn, J. Aerosol Sci. **20**, 367–380 (1989).
10. A.D. Gosman, W.M. Pun, A.K. Runchal, D.B. Spalding, and M.M. Wolfstein, *Heat and Mass Transfer in Recirculating Flow* (Academic Press, London, 1969).
11. K.R. May and R.C. Clifford, Ann. Occup. Hyg. **10**, 83–95 (1967).